Science of the Total Environment 646 (2019) 696–703

Contents lists available at ScienceDirect

Science of the Total Environment

journal homepage: www.elsevier.com/locate/scitotenv

Cadmium stable isotope variation in a mountain area impacted by acid mine drainage

Wen-Jun Yang [a,b], Keng-Bo Ding [a,b], Peng Zhang [a,b], Hao Qiu [c,*], Christophe Cloquet [d], Han-Jie Wen [e], Jean-Louis Morel [f], Rong-Liang Qiu [a,b], Ye-Tao Tang [a,b,**]

[a] School of Environmental Science and Engineering, Sun Yat-sen University, Guangzhou 510275, PR China
[b] Guangdong Provincial Key Laboratory of Environmental Pollution Control and Remediation Technology, Sun Yat-sen University, Guangzhou 510275, PR China
[c] School of Environmental Science and Engineering, Shanghai Jiao Tong University, Shanghai 200240, PR China
[d] CRPG-CNRS, Université de Lorraine, 15 rue Notre-Dame-des-Pauvres BP 20, 54501 Vandoeuvre lès Nancy, France
[e] State Key Laboratory of Ore Deposit Geochemistry, Institute of Geochemistry, Chinese Academy of Sciences, Guiyang 550081, PR China
[f] Université de Lorraine, INRA, Laboratoire Sols et Environnement, BP 172, 2 avenue de la forêt de Haye, F-54505 Vandoeuvre-lès-Nancy Cédex, France

HIGHLIGHTS

- Mineral, tailings, sediments and AMD-contaminated river water were analyzed for Cd isotope ratios.
- Distinctive Cd isotope signatures associated with transport and fate of riverine Cd.
- Agricultural activities contributed a heavy isotope signature input of Cd.
- Cadmium stable isotope is a promising tracer of attenuation processes in acid mine drainage.

GRAPHICAL ABSTRACT

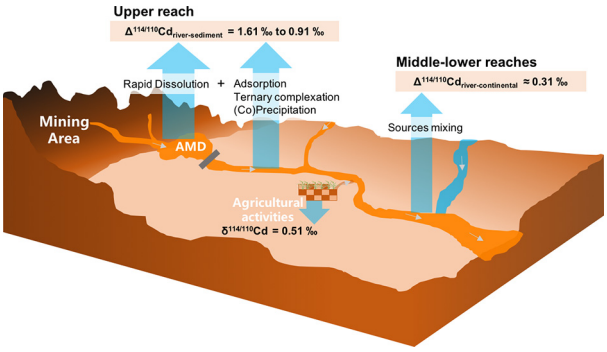

ARTICLE INFO

Article history:
Received 28 April 2018
Received in revised form 14 July 2018
Accepted 16 July 2018
Available online xxxx

Editor: Xinbin Feng

Keywords:
Cadmium isotope
Rivers
Trace metal
Source
Acid mine drainage

ABSTRACT

The pollution of natural waters and sediments with metals derived from acid mine drainage (AMD) is a global environmental problem. However, the processes governing the transportation and transformation of AMD metals such as Cd in mountainous areas are poorly understood. In this study, the Cd isotopic composition and Cd concentration of river water and sediments (16 sampling sites) from an AMD-affected river in southern China were determined. Cd concentration in river water declined from its source at a tailings dam (304 μg L^{-1}) to a point 14 km downstream (0.32 μg L^{-1}). Sediment Cd concentration ranged from 0.18 to 39.9 μg g^{-1}, suggesting that anthropogenic Cd is derived primarily from the tailing dam and easily enters the solid phase of the river. Isotopic data showed that the dissolved Cd in rivers was characterized by $\delta^{114/110}$Cd values ranging from 0.21‰ to 1.03‰, with a mean of 0.48‰. The greatest Cd isotope difference was observed between the water and sediments in the LW dam ($\Delta^{114/110}Cd_{river\text{-}sediment}$ = 1.61‰, site 1), likely due to a rapid weathering dissolution of the ore tailings. In the river's upper reach (sites 2–3), isotope difference between river and sediment ($\Delta^{114/110}Cd_{river\text{-}sediment}$) ranged from 1.0‰ to 0.91‰. This suggests that a host of secondary processes might have impacted Cd isotope fractionation, including adsorption, ternary complexation and/or (co)precipitation of Cd on secondary oxides and hydroxides. In the middle and lower reaches, an abruptly elevated $\delta^{114/110}$Cd value near farmland (site 10) suggests the existence of a second Cd source. Based on the chemical properties of

* Corresponding author.
** Correspondence to: Y.-T. Tang, School of Environmental Science and Engineering, Sun Yat-sen University, Guangzhou 510275, PR China.
E-mail addresses: haoqiu@sjtu.edu.cn (H. Qiu), eestyt@mail.sysu.edu.cn (Y.-T. Tang).

https://doi.org/10.1016/j.scitotenv.2018.07.210

water samples we can attribute this heavy isotope signature to agricultural fertilizer and drainage from agricultural fields. Our results suggest that Cd isotope is a tracer for identifying and tracking Cd sources and attenuation mechanisms (adsorption/(co)precipitation) in a complex mountain watershed.

1. Introduction

Cadmium (Cd) is a trace element that naturally occurs in the environment at levels of parts per billion. Cadmium and its compounds are highly toxic, carcinogenic, and can eventually enter the food chain and pose a serious threat to human health (Nordberg, 2009). Cadmium mineral deposits are rare, and the element often occurs as an isomorphic substituent in minerals found in primary ores of Fe, Pb, and especially Zn (*e.g.*, sphalerite) (Cullen and Maldonado, 2013). Metal sulfide deposits are common in many mountain regions and are often associated with extensive zones of pyritic alteration (Borrok et al., 2009). Weathering of metal sulfide deposits and historical mining activities generate acid mine drainage (AMD), a sulfuric acid-rich solution with low pH and a high content of toxic metals (Aranda et al., 2012). This acid flow enables heavy metals like Cd to be mobilized from mine wastelands (*e.g.* tailings) into their surrounding rivers (Dold, 2014). Anthropogenic activity is the primary source of the release of Cd, which can contribute over 0.64 t Cd to the surface water environment each year (Mayes et al., 2010). Because of difficulty of access and scarcity of monitoring equipment in areas with complex topography, the (bio)geochemical processes that control the mobility of metals such as Cd in mountain regions are hardly investigated.

Several investigations have demonstrated that isotopic signatures of Cu, Fe, and Zn vary substantially between natural and contaminated water pools (Balistrieri et al., 2008; Chen et al., 2009; Chen et al., 2014). Those isotopes have emerged as a useful tool for identifying both the sources of heavy metals in terrestrial environments and the main processes controlling the fate of those metals (Szynkiewicz and Borrok, 2016; Wiederhold, 2015). The adsorption or complexation of metals (*e.g.*, Zn) on biotic and abiotic surfaces, (co)precipitation with oxides/oxyhydroxides, and biological uptake can influence the isotope composition of dissolved metals (Aranda et al., 2012; Borrok et al., 2008; Borrok et al., 2009; Kimball et al., 2009). Previous studies have reported Cd isotope fractionation during Cd adsorption and precipitation on minerals, and heavier Cd isotopes are preferential remained in aqueous solutions (Horner et al., 2011; Wasylenki et al., 2014). In a microbial Cd uptake experiment, Cd bound in the cell membrane exhibited light Cd isotopic compositions as a result of sequestration of Cd in cell membrane (Horner et al., 2013). Considerable variation in the isotopic signature of Cd has been observed in seawater from several ocean regions, and Cd isotope fractionation is strongly controlled by biological processes (Abouchami et al., 2011; Abouchami et al., 2014; Gault-Ringold et al., 2012; Horner et al., 2013; Lacan et al., 2006; Ripperger et al., 2007; Xue et al., 2013). A study of the isotopic composition of Cd in the mixing zone of Siberian river estuaries found that the riverine input of several branch rivers had significantly different Cd isotope signatures (Lambelet et al., 2013). So far most researches on Cd isotopes in terrestrial systems have focused on industrial (Chrastný et al., 2015; Cloquet et al., 2006; Martinková et al., 2016; Shiel et al., 2010) and agricultural pollution (Imseng et al., 2018; Salmanzadeh et al., 2017; Wiggenhauser et al., 2016). However, we know very little about the direction and magnitude of isotopic changes of Cd that might occur as a result of specific geochemical processes in AMD polluted areas. In this study, we used stable isotope ratios of Cd combined with other geochemical tools to investigate Cd sources, transport, and attenuation in contaminated waters and sediments of a typical AMD-affected mountain area in south China.

2. Materials and methods

2.1. Study site and sampling procedure

Dabao mountain (24°33′39″N, 113°42′57″E) (Fig. 1) is located at northern Guangdong Province in southern China. The region has a humid subtropical climate with average annual temperature of 20 °C and annual rainfall of 1350–1750 mm. Since the 1970s, large scale mining for iron and copper ores has taken place in the area. In the current study, typical mineral samples (Fe sulfide-rich minerals) and mine tailings were collected from the mine area. A total of 16 river water samples and 16 sediment samples were collected from the Liwu (LW) tailings dam (the main source of AMD), the Hengshi (HS) River (contaminated by AMD), the Fandong (FD) River (a tributary of HS) and the Taiping (TP) River (a non-contaminated river). Sampling sites were established using a Garmin global positioning system (GPS). Samples were collected from upper (sites 1–4), middle (sites 8–10), and lower (sites 11–13) reaches of the HS river in June 2016 (Fig. 1). Prior to sampling, water sample bottles were acid washed and rinsed three times with pure water. In all sites, five sub-samples were collected across the river to form a composite water sample to represent each sampling site. The sites for sediment sampling were located as close as possible to the water sampling sites. At each site, the top layer (0–3 cm) sediments were collected by using a grab sampler, and a composite sample was formed by a mixture of 5 sub-samples within 10 m^2 to represent each sampling site.

After sampling, the water samples were immediately split into two types and stored into 1 L polypropylene bottles in the icebox. 1) dissolved water samples filtered through 0.45 μm cellulose acetate filter (Sartorius Stedim Biotech, Germany), and 2) unfiltered water samples that contained water and suspended particulate matter (SPM) (Kimball et al., 2009; Szynkiewicz and Borrok, 2016). Water samples for cation and isotopic ratio analysis were acidified to pH < 2 with sub-boiling distillation 14 M HNO_3, and for NO_3^- and SO_4^{2-} anion analysis were unacidified (filtered). Water quality parameters, including pH, EC, Eh and temperature were measured when sampling by using a calibrated multiparameter instrument (HYDROLabDS5, USA). All the samples were transported to the laboratory within 12 h. Then water and sediment samples were refrigerated at 4 °C and −18 °C before analysis. In order to present selected chemistry results graphically as a function of their sampling locations, the distance of each sampling site from the outlet of the LW dam was measured (Fig. 1).

2.2. Geochemical analysis

Sample preparation was conducted in a clean room facility. All acids used in this study were purified by sub-boiling distillation and the deionized water was >18.2 MΩ-grade purified from a Milli-Q water purification system (Millipore, Bedford, USA). For sediment samples, 50–100 mg was weighed into a 10-mL polytetrafluoroethylene (PTFE) bomb, and approximately 1 mL concentrated HNO_3 and 1 mL concentrated HF were added. The digestion was carried out at 190 °C for 2 days to remove organic material in the solid phase. Subsequently, each sample was taken to dryness at 120 °C, and the residue was dissolved in 1 mL concentrated HNO_3 and 1 mL H_2O and placed in a sealed bomb and digested at 190 °C for 24 h. After evaporation at 120 °C, the sample was dissolved in 2 mL of 2.0 M HCl, centrifuged at 5500 rpm

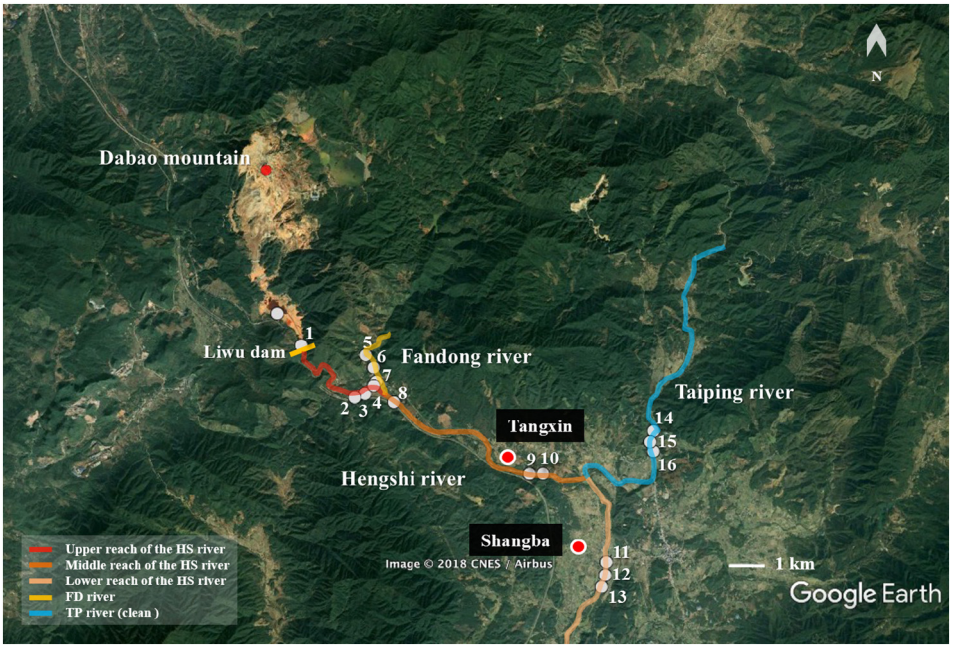

Fig. 1. Map of the AMD-affected area. Numbered dots show sampling locations at the Liwu dam and along the Hengshi, Fandong and Taiping rivers.

for 20 min, and was then ready for quantitative determination of Cd and other metals (k, Ca, Na, Mg, Al, Fe, Zn, Mn, Cu). For water samples, an aliquot of the river water was added into a 30-mL PTFE bomb and 1 mL concentrated HNO_3 and 1 mL concentrated HF were added. The digestion was carried out at 100 °C for 24 h to destroy organic materials. Subsequently, each sample was taken to dryness at 120 °C. The SO_4^{2-} anion concentration was measured by an ion chromatography (DX-600, Thermo Fisher). Major elements and trace elements concentrations for all water and digested samples were determined by ICP-OES (iCAP 6500 Duo, Thermo Fisher) and ICP-MS (ICAP Qc, Thermo Fisher). The Chinese National reference materials GSV-1 (bush branches and leaves) and GSD-12 (river sediments) purchased from Institute of Geophysical and Geochemical Exploration (IGGE), China, were used to check the precision and accuracy. The analytical results of Cd in GSV-1 and GSD-12 are in good agreement with the certified values, and the precision is better than 5% in terms of relative standard deviation (RSD). In addition, the mineralogy and morphology of all mineral and sediment samples were characterized by X-ray diffraction (XRD), X-ray fluorescence (XRF) and thermal field emission environmental scanning electron microscopy/energy dispersive X-ray spectrometry/electron backscatter diffraction (SEM/EDS/EBSD) at the Instrumental Analysis and Research Center, Sun Yat-Sen University (SYSU).

2.3. Cadmium isotope analysis

Sediment and filtered water samples were prepared for Cd isotope analysis according to anionexchange chromatographic method described in Cloquet et al. (2006) and Zhang et al. (2016). Macroporous anion-exchange resin AG-MP-1 M (0.7 g mL^{-1}, 100–200 mesh, chloride form) was purchased from Bio-Rad Laboratories. NIST 3108 Cd solution as a zero-delta isotope standard was purchased from NIST (Virginia, USA). Two secondary reference standard solutions - SPEX Cd (certiprep, Lot No: 7-27Cd) and Münster Cd (Wombacher and Rehkamper, 2004) were supplied by Dr. Cloquet at CRPG, France. Matrix components were separated from Cd on the AG-MP-1 M anion exchange resin, and the sample in 1 mL of 2 M HCl was loaded onto the washed and conditioned resin. The elution scheme for matrix removal was followed by 10 mL of 2 M HCl, 30 mL of 0.3 M HCl, 20 mL of 0.6 M HCl, and 5 mL of 0.012 M HCl. Then the final Cd was eluted in 20 mL of 0.0012 M HCl. Afterward the Cd fraction was dried and then re-dissolved in 1 mL 0.1 M HNO_3 with an ultrasonic bath for 30 min. A small amount of solution was collected before and after Cd purification for assessing Cd recovery and removal of the matrix. The recovery rates of Cd for GSV-1 and GSD-12 were higher than 97%. The recovery rates of isobaric interferences elements (*e.g.* Zn, Sn, In and Pd) were negligible. Cadmium isotopes were measured with a Neptune plus multi-collector ICP-MS instrument at the State Key Laboratory of Ore Deposit Geochemistry, Institute of Geochemistry, Chinese Academy of Sciences. The standard-sample-standard bracketing technique was applied for correction of instrumental mass bias. Between two and ten bracketed measurements of each sample were made depending on the stability of the MC-ICPMS (Cloquet et al., 2005). The isotopic composition of the samples is expressed in a delta per mill (‰) notation relative to the $Cd_{NIST\text{-}3108}$ reference solution according to the following equation:

$$\delta^{114/110}Cd = \left[\left(^{114/110}Cd\right)_{sample} / \left(^{114/110}Cd\right)_{standard} - 1\right] \times 1000$$

The isotopic fractionation between sediment and river water was calculated as:

$$\Delta^{114/110}Cd_{A-B} = \delta^{114/110}Cd_A - \delta^{114/110}Cd_B$$

where A and B represent the solid phases (*e.g.* sediment, tailing, mineral) and liquid phase (*e.g.* river water) in the AMD contaminated river system, respectively.

In order to directly compare the results from other laboratories, all isotopic results of this study are reported using a $\delta^{114/110}Cd$ notation, relative to the NIST 3108. $Cd_{Münster}$ and Cd_{spex} were regularly measured as secondary references throughout the study, which could provide a comparison of inter-laboratory quality control from different research institutes. In this study, we obtained a $\delta^{114/110}Cd_{Münster}$ value of 4.43 ± 0.06‰ (2SD, n = 10), a $\delta^{114/110}Cd_{spex}$ value of −0.07 ± 0.04‰ (2SD, n = 5). The measurements of GSD-12 yielded a $\delta^{114/110}Cd$ of 0.29 ± 0.05‰. These values are in good agreement with those previously published $\delta^{114/110}Cd_{spex} = -0.05 \pm 0.12$‰ and $\delta^{114/110}Cd_{Münster} = 4.40 \pm 0.04$‰ (Cloquet et al., 2005), $\delta^{114/110}Cd_{spex} = 0.01 \pm 0.12$‰ (Gao et al., 2008), and $\delta^{114/110}Cd_{Münster} = 4.50 \pm$

0.05‰ (Abouchami et al., 2013). The $\delta^{114/110}$Cd of river and sediment samples were determined in analytical duplicate in this case. The values were defined to be statistically different between the two samples if the mean values showed no overlap within the 2SD error bars. The uncertainty reported was expressed as 2SD from the mean of all the bracketed measurements.

3. Results and discussion

3.1. Geochemical characteristics of AMD-affected rivers

The LW dam is an open tailings dam built for containing drainage from the surrounding Fe sulfide-rich minerals and mining waste residues (Table S2). The water in the flooded area of the dam is primarily rainfall and runoff which have a high volume of AMD and suspended materials. The water at the exit of the dam was acidic, with pH values of 3.3 (Table 1). While the pH of surface water in the FD river was 4.1 to 4.2, slightly higher than that of the middle reach of the HS river (pH ranging from 3.7 to 4.1). The water collected from the TP river had a mean pH level of 7.6. In general, the concentrations of major ions such as iron (Fe), calcium (Ca), magnesium (Mg) and sulfate (SO_4^{2-}) in the HS river were highest at the LW dam (site 1). They decreased with increasing distance at the downstream sites, *e.g.* near the farmland of Tangxin village in the middle reach (sites 9 and 10) and near Shangba village in its lower reach (sites 11–13) (Fig. 2a). Similarly, water at the LW dam had the highest concentration of Zn, Mn and Cu (Fig. 2b). An exception occurred in the upper reach of the HS river (sites 2–4), where the highest SO_4^{2-} concentrations were observed at sites 3 and 4, but the Fe concentrations were markedly decreased at sites 2 and 3 (Fig. 2a). This is likely because of the presence of high oxygen content and Eh in the water (Table 1) and therefore a rapid formation of Fe (III) minerals (Fiedler et al., 2007; Patrick and Jugsujinda, 1992). It is commonly believed that the (oxy)hydroxides of Al and Fe are ubiquitous in the environment. They release to solution from primary mineral dissolution and tend to precipitate from solution in the form of aluminum and iron-bearing secondary minerals (Collignon et al., 2012). Due to long-term flooding and a low pH environment, primary minerals like pyrite/pyrrhotite (light and thin section in Fig. S1, a, c) in the sediment of LW dam site were completely dissolved (Fig. S1 e and f). SPM in water samples was high in Fe and Al (Fig. 3), which contributed to formation of secondary minerals in sediments of the lower reaches (Table 1). It is expected that secondary minerals would play an important role in the geochemical processes controlling transport of Cd in the AMD polluted river system.

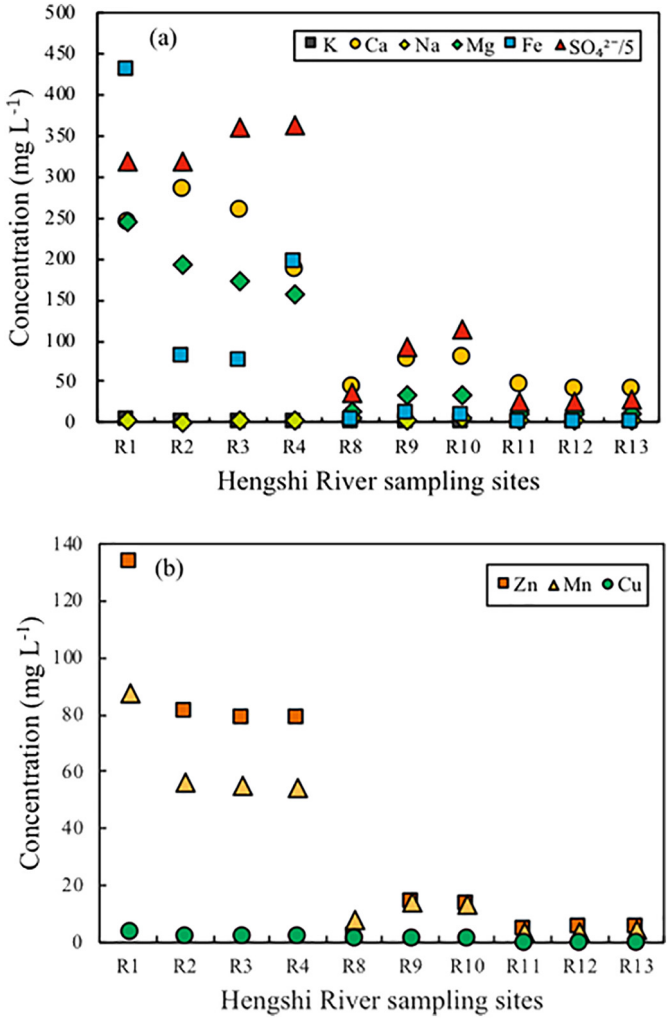

Fig. 2. Major (a) and trace (b) element concentrations in the AMD-affected Hengshi River (filtered).

3.2. Cd concentration of stream and sediment samples

Cd concentrations in river water ranged from 304 μg L^{-1} at the LW dam to 0.32 μg L^{-1} at site 14 of the uncontaminated TP river

Table 1
Cd concentration and isotope composition (as $\delta^{114/110}Cd_{NIST\ 3108}$) of samples; chemical characteristics of sediment and river water.

Sample site	pH	Eh (mV)	NH_4^+ (mg L^{-1})	NO_3^- (mg L^{-1})	Sal (‰)	DO (mg L^{-1})	Cd (μg L^{-1})	$\delta^{114/110}$Cd (‰)	Fe (%)	Al (%)	S (%)	Cd (μg g^{-1})	$\delta^{114/110}$Cd (‰)
	River water								Sediment				
1	3.33	457	3.81	0.41	1.82	5.01	304.2	0.64 ± 0.03	10	2.18	0.69	1.27	−0.97 ± 0.09
2	3.57	518	3.92	0.47	1.87	6.54	191.7	1.03 ± 0.02	24	2.82	3.15	39.9	0.03 ± 0.03
3	3.45	518	4.02	0.44	1.82	6.47	183.3	0.94 ± 0.03	21	2.59	3.06	38.6	0.03 ± 0.06
4	3.31	520	4.42	0.40	0.29	6.52	181.1	0.80 ± 0.06	15	1.77	1.67	14.1	ND
5	4.14	334	3.62	0.26	0.17	6.96	14.82	0.38 ± 0.00	7.8	1.07	0.18	0.18	ND
6	4.24	332	3.92	0.30	0.26	5.71	16.02	0.21 ± 0.07	5.8	1.38	0.20	0.26	ND
7	4.15	334	3.75	0.32	0.30	6.43	12.90	0.33 ± 0.03	6.8	1.50	0.31	0.21	ND
8	4.08	332	3.85	0.29	0.68	7.30	13.76	0.35 ± 0.01	8.6	2.55	0.50	4.85	ND
9	3.72	356	4.02	1.59	0.62	6.18	40.62	0.30 ± 0.02	16	1.84	1.49	2.19	ND
10	3.72	593	9.38	35.95	0.13	6.13	37.64	0.51 ± 0.03	26	1.88	2.87	1.36	ND
11	5.20	288	3.96	10.23	0.23	5.14	13.22	0.25 ± 0.00	12	1.75	0.36	1.47	ND
12	4.57	251	4.52	6.65	0.22	6.38	13.74	0.23 ± 0.04	13	3.29	0.99	2.03	ND
13	5.16	328	4.77	2.81	0.10	7.24	14.10	0.25 ± 0.00	16	3.50	1.62	1.81	ND
14	7.77	57	4.03	4.93	0.11	7.49	0.32	ND	2.7	2.17	0.16	0.53	ND
15	7.66	89	3.93	4.37	0.11	6.68	0.41	ND	2.5	2.21	0.03	0.25	ND
16	7.50	76	4.00	6.05	1.82	6.30	0.41	ND	3.1	1.89	0.03	0.74	ND

Sal: salinity. DO: dissolved oxygen. ND: not determined.
The uncertainty reported was expressed as 2SD based on repeated measurements.

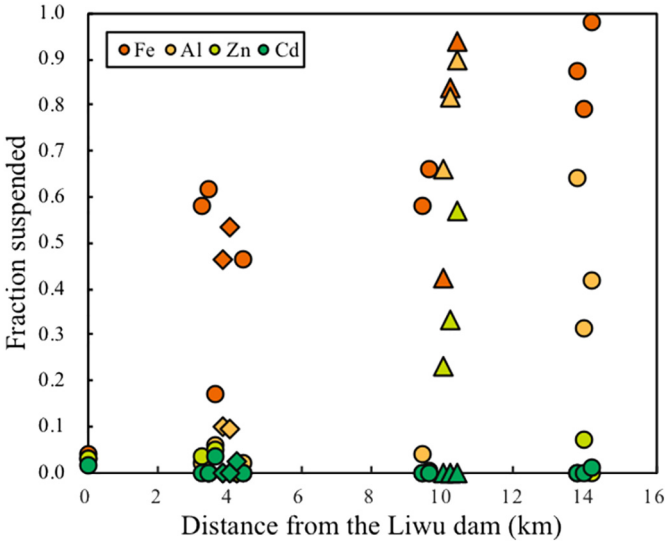

Fig. 3. Fractions of Fe, Al, Cd and Zn in the suspended (*i.e.*, particulate) load of surface water samples relative to total Fe, Al, Cd and Zn concentrations. Distances are measured arbitrarily relative to the outlet of the Liwu dam. ○ Circles: Hengshi River; ◇ Diamonds: Fandong River; △ Triangles: Taiping River.

(Table 1), ranging from 304 to 13.22 μg L^{-1} in the HS river and from 16.0 to 12.9 μg L^{-1} in the FD river and from 0.41 to 0.32 μg L^{-1} in the TP river. The historically dispersed illegal mining pits in Dabao mountain mine area, in combination with severe soil erosion, significantly decreased the pH and contributed high concentration of Cd to the FD river. The TP river had a good water quality which was not impacted by mining activity. In HS river water, dissolved Cd concentration decreased with the increasing distance from the LW dam and remained as dissolved Cd (Fig. 4a). Cadmium concentrations in sediments ranged from 1.27 to 39.9 μg g^{-1} in the HS river and from 0.18 to 0.74 μg g^{-1} in its tributaries (Table 1). This attenuation is likely controlled by a variety of geochemical processes and hydrological conditions such as adsorption or (co) precipitation, by which dissolved Cd can easily enter the sediment phase. The fate of Cd is generally controlled by its chemical speciation and riverine oxy(hydr)oxides (Cullen and Maldonado, 2013). Previous studies have shown that Cd were present as free Cd^{2+} ions and Cd^{2+}-sulfate complexes under the prevailing acid conditions (Yu and Patrick, 2003). In this situation, Cd was maintained as dissolved throughout its migration to the lower reaches of the river. For the sediments, although the LW dam (site 1) contained all the tailings and mining waste residues, it showed a low Cd concentration of 1.27 μg g^{-1} compared to other sites in the upper reach. Cd concentrations in the sediments at sites 2–4 ranged from 14.1 to 39.9 μg g^{-1}, much higher than those of other sites (Table 1). XRD spectra showed very low peaks and smooth spectral lines of these sediments of sites 2–4 (Fig. S3), suggesting formation of weakly crystalline and/or amorphous minerals. The sediments of upper reach sites were also rich in high Fe content that could easily form weakly crystalline and/or amorphous Fe-rich minerals (Table 1). The weakly crystalline minerals are characterized of high metal (*e.g.* Cd) binding capacity as increasing surface area of the minerals (Song et al., 2008), even under acidic conditions (Zhu et al., 2016). Previous studies found that under the AMD environment, a Cd-ternary complex formed on the surface of ferrihydrite and goethite in the presence of high SO_4^{2-} (Song et al., 2008; Swedlund et al., 2009). That is why sediments of sites 2–4 could trap more Cd than other sites (Table 1). An exception to the Cd attenuation trend was observed at sites 9 and 10, where the river Cd concentration was three times that of their upstream site 8 and downstream sites (Table 1). At site 10, the elevated concentrations of NH_4^+ and NO_3^+ as well as elevated Eh and EC values (Table 1), suggests an additional input of Cd in this area.

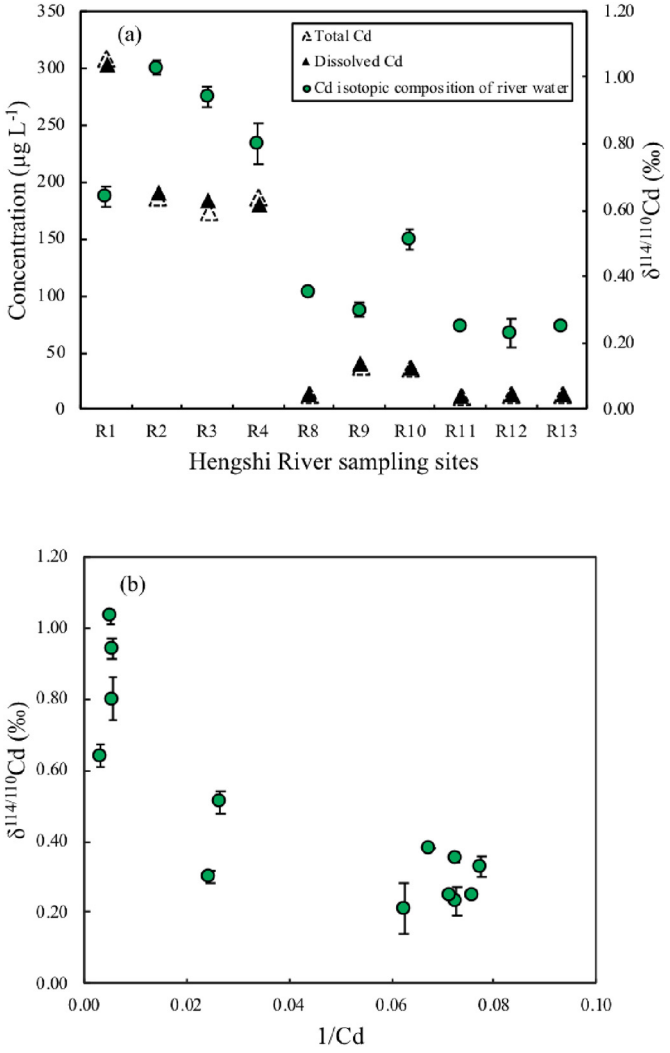

Fig. 4. (a) Left axis: dissolved and total Cd concentrations in river water samples from the AMD-affected Hengshi River; right axis: Cd isotopic composition of river water samples (filtered). (b) Cd isotopic composition *versus* the inverse Cd concentration (μg L^{-1}) of river water samples (filtered). Error bars are 2σ uncertainties based on repeated measurements.

3.3. Cd isotope signatures and fractionation in the AMD contaminated river

3.3.1. Cd isotope fractionation in the upper reach

The Cd isotopic composition ($\delta^{114/110}Cd$) of filtered river water ranged from 0.21‰ to 1.03‰ (Fig. 4b) with a mean of 0.48‰. At the LW dam (site 1), which had the highest concentrations of Cd, the $\delta^{114/110}Cd$ of water was 0.64 ± 0.03‰. Sites 2–4, which were located along the upper reach of the HS river, had the highest $\delta^{114/110}Cd$ values (0.80 to 1.03‰). At site 1, the Cd isotope composition of the tailings (−0.97 ± 0.09‰) was very similar to that of Fe sulfide-rich minerals (−0.95 ± 0.12‰) (Table S2), indicating that they are derived from a same Cd source. Yang et al. (2015) have reported light Cd isotope enrichment in cadmium hydrosulfide than other cadmium complexes by density functional theoretical calculations. Schmitt et al. (2009) found that Cd isotope compositions of several hydrothermal sulfides ranged from −0.65 to 0.19‰. Therefore, the light Cd isotope signature in Fe sulfide-rich minerals seem to be controlled by Cd species and mineralization mechanism during ore-formation processes in hydrothermal system. At sites 2 and 3, the sediment samples yielded a near-zero $\delta^{114/110}Cd$ value (Table 1), resulting in decreasing isotope difference between river water and sediment ($\Delta^{114/110}Cd_{river\text{-}sediment}$ = 0.91‰)

compared to site 1 ($\Delta^{114/110}Cd_{river\text{-}sediment} = 1.61‰$). During this transportation of Cd in the upper reach of the HS river, a marked decrease in Cd concentration from 304 to 181 μg L^{-1} was observed. However, the concentration of Fe decreased at sites 2–3, then increased at site 4 (Fig. 2a, 4a). At sites 2–4, the sediments were enriched much higher concentration of Cd than that of other sites (Table 1), which implies that Cd migrates from liquid phase into the solid phase by adsorption or (co)precipitation.

Recently, a number of studies have reported a heavy Cd isotopic signature of seawater (Abouchami et al., 2011; Janssen et al., 2017; Xue et al., 2013). The study of Cd isotopes in the Siberian estuary zone of the Arctic Ocean showed that the river water is slightly enriched in heavy Cd isotopes compared to the continental crust ($\Delta^{114/110}Cd_{river\text{-}continental\ crust} < 0.2‰$) (Lambelet et al., 2013). Cd isotopic composition of average bulk continental crust is $\delta^{114/110}Cd = -0.01 \pm 0.04‰$ (Schmitt et al., 2009). This implies that Cd isotope fractionation during weathering is either minor or insignificant. However, it has not been reported for the Cd isotopes in terrestrial riverine waters, especially the river impacted by AMD. In our study, the dissolved Cd of the rivers was obviously heavier than the continental crust ($\Delta^{114/110}Cd_{river\text{-}continental\ crust} > 0.4‰$), implying that Cd isotope fractionation during weathering was non-negligible.

In a first step, Cd isotopic composition of river water is largely dominated by weathering dissolution of Cd-bearing minerals that releases Cd from the solid phase into the liquid phase. The $\delta^{114/110}Cd$ *vs* 1/Cd data of water (Fig. 4b) suggests one of the sources stemmed from LW dam which had distinct Cd isotopic signatures. Previous studies showed that simulated oxidative weathering of sulfide minerals and rocks can produce $\Delta^{114/110}Cd_{solution\text{-}mineral}$ up to 0.53‰ (Zhang et al., 2016). In addition, natural weathering dissolution of Cd-bearing minerals (hydrozincite, smithsonite and angleite) can result in $\Delta^{114/110}Cd_{solution\text{-}mineral}$ up to 0.33‰ (Zhu et al., 2018). This fractionation might be related to an incongruent dissolution of different Cd-containing minerals by a galvanic effect (Acero et al., 2007; de Livera et al., 2011). The galvanic effect often occurs when two sulfide minerals with different rest potentials are coupled together. The mineral with the higher rest potential (*e.g.* pyrite as a cathode) could dissolve firstly and the lower rest potential (*e.g.* sphalerite) is protected (Acero et al., 2007; de Livera et al., 2011; Qian et al., 2018). Hence, if the continuous weathering dissolution of tailings is the main process for Cd isotope fractionation, it still cannot account for the $\Delta^{114/110}Cd_{river\text{-}tailing}$ (up to 1.6‰) observed in the upper reach rive. This implies that other processes might also play a role in this circumstance, *e.g.* adsorption and (co)precipitation on minerals.

Wasylenki et al. (2014) observed a large fractionation during Cd adsorption to birnessite. Initially, the Cd isotope fractionation between solution and solid phases was up to 0.8‰ at a high ionic strength, but decreased to 0.4‰ in the course of the experiment. This suggests that both equilibrium and kinetic processes play a role in the different stages of adsorption process. As to precipitation process, Horner et al. (2011) reported a large fractionation ($\Delta^{114/110}Cd_{solution\text{-}calcite} = 0.45 \pm 0.12‰$) between solution and precipitated calcite at high ionic strength. The lighter isotope of Cd is preferentially incorporated into the mineral phase due to kinetic isotope fractionation. And the return of Cd to solution phase is likely minor with developed crystal-growth. Meanwhile, as ferrihydrite and goethite are commonly found in the sediments of AMD-polluted rivers (Fig. S1–S3) (Silva et al., 2013), it is expected that Cd in the sediments be immobilized by co-precipitation and adsorption. In this work, sulfate was the major dissolved anion (Fig. 2a and Table 1) and had strong complexation ability to Fe secondary mineral. The high content of sulfate could inhibit Fe(III) hydrolysis to form the weakly crystalline iron oxides (Schwertmann and Cornell, 2008). Furthermore, it has been shown that sulfate formed both outer- and inner-sphere complexes on minerals at acidic condition (Zhu et al., 2016). These factors have enabled the opportunity to adsorb more Cd in sites 2–4 (Table 1). During the early stages of the formation of secondary minerals, Cd may enter into solid phase by rapid (co)precipitation onto/with Fe (oxy)hydroxides, and is further preserved into mineral lattice even in extremely acidic conditions (Jiang et al., 2013). It is also favorable for formation of ternary complexation with more Cd on minerals surface, suggesting that stiffer Cd-ligand aqueous complexes also form stronger surface ternary complexes by calculating the ternary complex formation constants (Swedlund et al., 2009). This ternary complex formation on goethite could generate $\Delta^{114/110}Cd_{solution\text{-}solid}$ up to 0.61‰ (unpublished data). Accordingly, these implications could be used to explain why the upper reach had much higher $\delta^{114/110}Cd$ than the middle and lower reaches in this scenario.

3.3.2. Cd isotope fractionation in the middle and lower reaches

After entering the middle and lower reaches, the $\delta^{114/110}Cd$ value of stream river samples (sites 5–13) varied in the range of 0.21‰ to 0.51‰ (Fig. 4b), approximately the same variation (0.31‰) between the river water and the bulk continental crust (Schmitt et al., 2009). This fractionation is similar in magnitude to the isotopic variation observed for

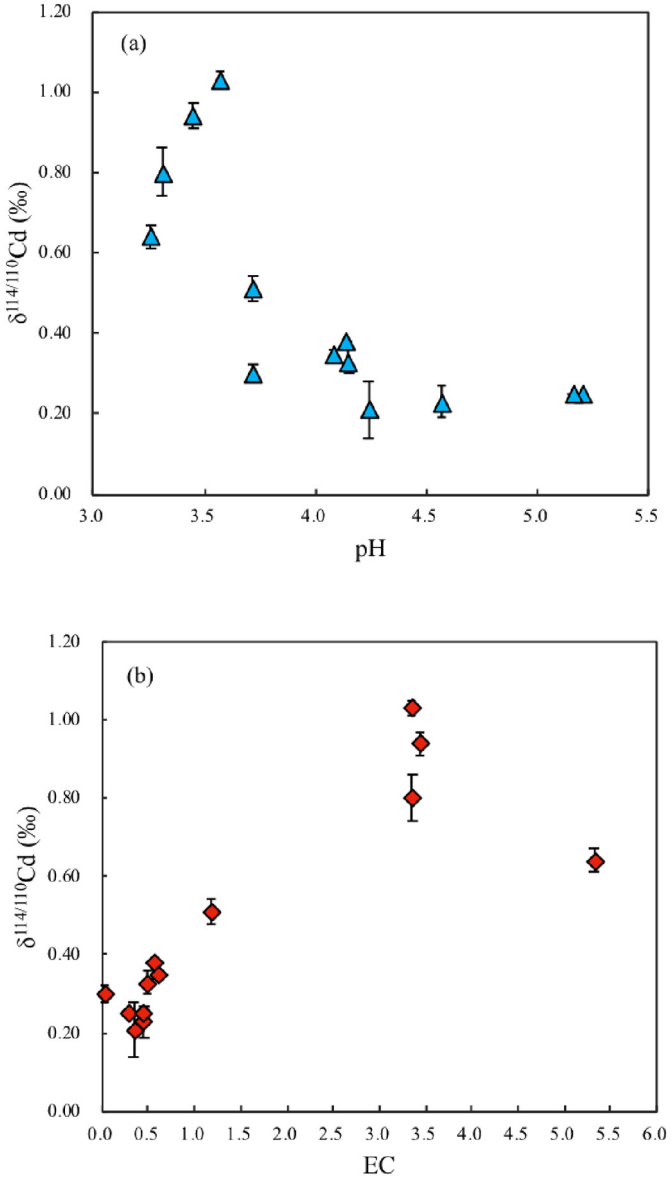

Fig. 5. (a) Cd isotopic composition *versus* the pH of river waters (filtered). (b) Cd isotopic composition *versus* the EC (mS cm^{-1}) of river waters (filtered). Error bars are 2σ uncertainties based on repeated measurements.

natural weathering of sulfide mineral, *i.e.* $\Delta^{114/110}Cd_{solution\text{-}mineral} = 0.33‰$ (Zhu et al., 2018).

As a consequence of the waters being diluted and neutralized, the composition of $\delta^{114/110}Cd$ declined with the increase of the pH of river (Fig. 5a). This is consistent with the fact that the ionic strength of the river waters, which was dominated by electrical conductivity and salinity, decreased substantially from upstream to the downstream (Table 1). Results also showed that the Cd isotope signature changed with the electrical conductivity of the river waters (Fig. 5b). It has been shown that the dissolved Cd may exchange completely with the sorbed Cd in a short period, achieving a smaller fractionation of $\Delta^{114/110}Cd_{solution\text{-}mineral} = 0.24‰$ at low ionic strength than at high ionic strength (Wasylenki et al., 2014). Using density functional theoretic calculation, Yang et al. (2015) found that the fractionation was caused by the changes of Cd ligand between different Cd complexes. Another reason for the fractionation is ascribed to the transformation of the poorly crystalline ferrihydrite into the ordered goethite resulting from dehydration (Boland et al., 2014). The distinct transformation of surface structure is also accompanied by a decrease in total surface area and changes in adsorption sites, which may influence the formation of ternary complexation with Cd (Swedlund et al., 2009). This change in number of adsorption sites would make Cd re-distribute at the solid-liquid interface and thus would have an impact on the isotope composition variation of Cd.

3.4. An additional Cd source from agricultural activity?

A heavier Cd isotopic signature ($\delta^{114/110}Cd = 0.51 \pm 0.03‰$) was found in the water sample at the site 10 compared to neighboring sampling sites, which was located near farmland in the middle reach of the HS river (Fig. 4a). There has been some research on Cd isotope fractionation associated with agricultural activities such as irrigation with contaminated water and fertilization. For instance, in a soil-wheat system, Wiggenhauser et al. (2016) found that the $Ca(NO_3)_2$-extracted Cd from soil was isotopically heavier than the total Cd in the soil ($\Delta^{114/110}Cd_{extract\text{-}soil} = 0.16$ to 0.45‰). Imseng et al. (2018) reported that the manure applied in arable soil had $\delta^{114/110}Cd$ values of 0.35 to 0.38‰, and Cd in seepage ($\delta^{114/110}Cd = 0.39$ to 0.79‰) was isotopically heavier than in the soil. Salmanzadeh et al. (2017) who investigated Cd isotopic compositions of fertilizer and soil samples from a 66-year-long field trial, also reported that the soils were enriched in heavy Cd isotopes regardless of mineral phosphate fertilizers used. These studies suggest that fertilizers and soil seepage might become an important Cd input into rivers and groundwater. In the present study, Cd minerals were not detected in river sediment by XRD (Fig. S3), probably because of the aerobic and acidic environment (Table 1). This excludes the possibility of Cd isotope fractionation during the formation of Cd secondary minerals. Furthermore, we also found elevated concentrations of NH_4^+ (7.53 to 11.58 mg L^{-1}) and NO_3^+ (35.95 to 277 mg L^{-1}) as well as elevated Eh and EC values at site 10 and site TX (Table 1and Table S1), which was about two times higher for NH_4^+ and much higher for NO_3^+ than any other sites in HS river. This phenomenon of nitrate and ammonium losses from agricultural activities have been attributed to inorganic and organic fertilizers (King and Torbert, 2007; Sebilo et al., 2013). Several studies have also highlighted different strategies to identify nitrate and ammonium pollution from agricultural runoff (Hao et al., 2018; Li et al., 2017; Yi et al., 2017). Thus, based on Cd isotopic signature and environmental characteristics, the peculiar Cd isotopic signature near Tangxin village implies that there is another source of Cd originating from agricultural activity.

4. Conclusions

In this study, the AMD contaminated river is characterized by significantly higher $\delta^{114/110}Cd$ compared to the first report of riverine water in the Siberian Shelf (Lambelet et al., 2013). The co-variation between the major element concentrations and Cd concentrations in the river water may be interpreted in terms of a similar geochemical behavior during transport processes that released Cd from tailing dam. The waters exhibit large and resolvable Cd isotopic variation with $\delta^{114/110}Cd$ values ranging from 0.21‰ to 1.03‰. Changes in $\delta^{114/110}Cd$ could be predominantly attributed to conservative mixing of isotopic distinct HS river and its tributary FD river, and certain in-stream geochemical processes. In the upper reach of the HS river, the highest Cd isotope difference between river water and sediments ($\Delta^{114/110}Cd_{river\text{-}sediment} = 0.91$ to 1.61‰) indicates the occurrence of weathering dissolution of sulfide-rich mine tailings, adsorption/(co)precipitation on secondary minerals, and probably the Cd-SO_4^{2-} ternary complexation. While in the middle and low reach, $\delta^{114/110}Cd$ values of river water (0.21‰ to 0.51‰) were approximately the same variation (0.31‰) between the river water and the bulk continental crust (Schmitt et al., 2009). Moreover, a peculiarly high $\delta^{114/110}Cd$ in the water at the middle reach, together with its elevated concentrations of NH_4^+ and NO_3^+, suggests another input of Cd from agricultural activities. All these features highlight that Cd isotope signature in such studies can be an useful tool to trace the source and identify the attenuation processes of Cd in the polluted aquatic environment, in addition to conventional geochemical method.

Acknowledgements

We thank Yuwei Su, Ting Zhou and Yuxu Zhang for technical support in ICP-MS and MC-ICPMS measurements. This work was financially supported by the National Key R&D Program of China (2018YFD0800700), the Natural Science Foundation of China (No. 41371315, No. 41225004, No. 41771343) and the 111 Project (B18060). We are grateful to the anonymous reviewers for their valuable comments and suggestions.

Appendix A. Supplementary data

Supplementary data to this article can be found online at https://doi.org/10.1016/j.scitotenv.2018.07.210.

References

Abouchami, W., Galer, S.J.G., de Baar, H.J.W., Alderkamp, A.C., Middag, R., Laan, P., et al., 2011. Modulation of the Southern Ocean cadmium isotope signature by ocean circulation and primary productivity. Earth Planet. Sci. Lett. 305, 83–91.

Abouchami, W., Galer, S.J.G., Horner, T.J., Rehkamper, M., Wombacher, F., Xue, Z.C., et al., 2013. A common reference material for cadmium isotope studies - NIST SRM 3108. Geostand. Geoanal. Res. 37, 5–17.

Abouchami, W., Galer, S.J.G., de Baar, H.J.W., Middag, R., Vance, D., Zhao, Y., et al., 2014. Biogeochemical cycling of cadmium isotopes in the Southern Ocean along the Zero Meridian. Geochim. Cosmochim. Acta 127, 348–367.

Acero, P., Cama, J., Ayora, C., 2007. Sphalerite dissolution kinetics in acidic environment. Appl. Geochem. 22, 1872–1883.

Aranda, S., Borrok, D.M., Wanty, R.B., Balistrieri, L.S., 2012. Zinc isotope investigation of surface and pore waters in a mountain watershed impacted by acid rock drainage. Sci. Total Environ. 420, 202–213.

Balistrieri, L.S., Borrok, D.M., Wanty, R.B., Ridley, W.I., 2008. Fractionation of Cu and Zn isotopes during adsorption onto amorphous Fe(III) oxyhydroxide: experimental mixing of acid rock drainage and ambient river water. Geochim. Cosmochim. Acta 72, 311–328.

Boland, D.D., Collins, R.N., Miller, C.J., Glover, C.J., Waite, T.D., 2014. Effect of solution and solid-phase conditions on the Fe(II)-accelerated transformation of ferrihydrite to lepidocrocite and goethite. Environ. Sci. Technol. 48, 5477–5485.

Borrok, D.M., Nimick, D.A., Wanty, R.B., Ridley, W.I., 2008. Isotopic variations of dissolved copper and zinc in stream waters affected by historical mining. Geochim. Cosmochim. Acta 72, 329–344.

Borrok, D.M., Wanty, R.B., Ridley, W.I., Lamothe, P.J., Kimball, B.A., Verplanck, P.L., et al., 2009. Application of iron and zinc isotopes to track the sources and mechanisms of metal loading in a mountain watershed. Appl. Geochem. 24, 1270–1277.

Chen, J., Gaillardet, J., Louvat, P., Huon, S., 2009. Zn isotopes in the suspended load of the Seine River, France: isotopic variations and source determination. Geochim. Cosmochim. Acta 73, 4060–4076.

Chen, J.-B., Busigny, V., Gaillardet, J., Louvat, P., Wang, Y.-N., 2014. Iron isotopes in the Seine River (France): natural versus anthropogenic sources. Geochim. Cosmochim. Acta 128, 128–143.

Chrastný, V., Čadková, E., Vaněk, A., Teper, L., Cabala, J., Komárek, M., 2015. Cadmium isotope fractionation within the soil profile complicates source identification in relation to Pb–Zn mining and smelting processes. Chem. Geol. 405, 1–9.
Cloquet, C., Rouxel, O., Carignan, J., Libourel, G., 2005. Natural cadmium isotopic variations in eight geological reference materials (NIST SRM 2711, BCR 176, GSS-1, GXR-1, GXR-2, GSD-12, Nod-P-1, Nod-A-1) and anthropogenic samples, measured by MC-ICP-MS. Geostand. Geoanal. Res. 29, 95–106.
Cloquet, C., Carignan, J., Libourel, G., Sterckeman, T., Perdrix, E., 2006. Tracing source pollution in soils using cadmium and lead isotopes. Environ. Sci. Technol. 40, 2525–2530.
Collignon, C., Ranger, J., Turpault, M.P., 2012. Seasonal dynamics of Al- and Fe-bearing secondary minerals in an acid forest soil: influence of Norway spruce roots (Picea abies (L.) Karst.). Eur. J. Soil Sci. 63, 592–602. https://doi.org/10.1111/j.1365-2389.2012.01470.x.
Cullen, J.T., Maldonado, M.T., 2013. Biogeochemistry of cadmium and its release to the environment. Met. Ions Life Sci. 11, 31–62.
de Livera, J., McLaughlin, M.J., Beak, D., Hettiarachchi, G.M., Kirby, J., 2011. Release of dissolved cadmium and sulfur nanoparticles from oxidizing sulfide minerals. Soil Sci. Soc. Am. J. 75, 842–854.
Dold, B., 2014. Evolution of acid mine drainage formation in sulphidic mine tailings. Fortschr. Mineral. 4, 621–641.
Fiedler, S., Vepraskas, M.J., Richardson, J., 2007. Soil redox potential: importance, field measurements, and observations. Adv. Agron. 94, 1–54.
Gao, B., Liu, Y., Sun, K., Liang, X., Pa, Peng, Sheng, G., et al., 2008. Precise determination of cadmium and lead isotopic compositions in river sediments. Anal. Chim. Acta 612, 114–120.
Gault-Ringold, M., Adu, T., Stirling, C.H., Frew, R.D., Hunter, K.A., 2012. Anomalous biogeochemical behavior of cadmium in subantarctic surface waters: mechanistic constraints from cadmium isotopes. Earth Planet. Sci. Lett. 341, 94–103.
Hao, Z., Zhang, X.Y., Gao, Y., Xu, Z.W., Yang, F.T., Wen, X.F., et al., 2018. Nitrogen source track and associated isotopic dynamic characteristic in a complex ecosystem: a case study of a subtropical watershed, China. Environ. Pollut. 236, 177–187.
Horner, T.J., Rickaby, R.E.M., Henderson, G.M., 2011. Isotopic fractionation of cadmium into calcite. Earth Planet. Sci. Lett. 312, 243–253.
Horner, T.J., Lee, R.B.Y., Henderson, G.M., Rickaby, R.E.M., 2013. Nonspecific uptake and homeostasis drive the oceanic cadmium cycle. Proc. Natl. Acad. Sci. U. S. A. 110, 2500–2505.
Imseng, M., Wiggenhauser, M., Keller, A., Muller, M., Rehkamper, M., Murphy, K., et al., 2018. Fate of cd in agricultural soils: a stable isotope approach to anthropogenic impact, soil formation, and soil-plant cycling. Environ. Sci. Technol. 52, 1919–1928.
Janssen, D.J., Abouchami, W., Galer, S.J.G., Cullen, J.T., 2017. Fine-scale spatial and interannual cadmium isotope variability in the subarctic northeast Pacific. Earth Planet. Sci. Lett. 472, 241–252. https://doi.org/10.1016/j.epsl.2017.04.048.
Jiang, W., Lv, J., Luo, L., Yang, K., Lin, Y., Hu, F., et al., 2013. Arsenate and cadmium co-adsorption and co-precipitation on goethite. J. Hazard. Mater. 262, 55–63.
Kimball, B.E., Mathur, R., Dohnalkova, A.C., Wall, A.J., Runkel, R.L., Brantley, S.L., 2009. Copper isotope fractionation in acid mine drainage. Geochim. Cosmochim. Acta 73, 1247–1263.
King, K., Torbert, H., 2007. Nitrate and ammonium losses from surface-applied organic and inorganic fertilizers. J. Agric. Sci. 145, 385–393.
Lacan, F., Francois, R., Ji, Y., Sherrell, R.M., 2006. Cadmium isotopic composition in the ocean. Geochim. Cosmochim. Acta 70, 5104–5118.
Lambelet, M., Rehkamper, M., de Flierdt, T.V., Xue, Z.C., Kreissig, K., Coles, B., et al., 2013. Isotopic analysis of Cd in the mixing zone of Siberian rivers with the Arctic Ocean-new constraints on marine Cd cycling and the isotope composition of riverine Cd. Earth Planet. Sci. Lett. 361, 64–73.
Li, J.Y., Tong, J.X., Xia, C.N., Hu, B.X., Zhu, H., Yang, R., et al., 2017. Numerical simulation and experimental study on farmland nitrogen loss to surface runoff in a raindrop driven process. J. Hydrol. 549, 754–768.
Martinková, E., Chrastný, V., Francová, M., Šípková, A., Čuřík, J., Myška, O., et al., 2016. Cadmium isotope fractionation of materials derived from various industrial processes. J. Hazard. Mater. 302, 114–119.
Mayes, W.M., Potter, H.A.B., Jarvis, A.P., 2010. Inventory of aquatic contaminant flux arising from historical metal mining in England and Wales. Sci. Total Environ. 408, 3576–3583.
Nordberg, G.F., 2009. Historical perspectives on cadmium toxicology. Toxicol. Appl. Pharmacol. 238, 192–200.
Patrick, W., Jugsujinda, A., 1992. Sequential reduction and oxidation of inorganic nitrogen, manganese, and iron in flooded soil. Soil Sci. Soc. Am. J. 56, 1071–1073.
Qian, G., Fan, R., Short, M.D., Schumann, R.C., Li, J., St, C., Smart, R., et al., 2018. The effects of galvanic interactions with pyrite on the generation of acid and metalliferous drainage. Environ. Sci. Technol. 52, 5349–5357.
Ripperger, S., Rehkaemper, M., Porcelli, D., Halliday, A.N., 2007. Cadmium isotope fractionation in seawater - a signature of biological activity. Earth Planet. Sci. Lett. 261, 670–684.
Salmanzadeh, M., Hartland, A., Stirling, C.H., Balks, M.R., Schipper, L.A., Joshi, C., et al., 2017. Isotope tracing of long-term cadmium fluxes in an agricultural soil. Environ. Sci. Technol. 51, 7369–7377.
Schmitt, A.D., Galer, S.J.G., Abouchami, W., 2009. Mass-dependent cadmium isotopic variations in nature with emphasis on the marine environment. Earth Planet. Sci. Lett. 277, 262–272.
Schwertmann, U., Cornell, R.M., 2008. Iron Oxides in the Laboratory. John Wiley & Sons.
Sebilo, M., Mayer, B., Nicolardot, B., Pinay, G., Mariotti, A., 2013. Long-term fate of nitrate fertilizer in agricultural soils. Proc. Natl. Acad. Sci. U. S. A. 110, 18185–18189.
Shiel, A.E., Weis, D., Orians, K.J., 2010. Evaluation of zinc, cadmium and lead isotope fractionation during smelting and refining. Sci. Total Environ. 408, 2357–2368.
Silva, L.F.O., Fdez-Ortiz de Vallejuelo, S., Martinez-Arkarazo, I., Castro, K., MLS, Oliveira, Sampaio, C.H., et al., 2013. Study of environmental pollution and mineralogical characterization of sediment rivers from Brazilian coal mining acid drainage. Sci. Total Environ. 447, 169–178.
Song, Y., Swedlund, P.J., Singhal, N., 2008. Copper(II) and Cadmium(II) sorption onto ferrihydrite in the presence of phthalic acid: some properties of the ternary complex. Environ. Sci. Technol. 42, 4008–4013.
Swedlund, P.J., Webster, J.G., Miskelly, G.M., 2009. Goethite adsorption of Cu(II), Pb(II), Cd (II), and Zn(II) in the presence of sulfate: properties of the ternary complex. Geochim. Cosmochim. Acta 73, 1548–1562.
Szynkiewicz, A., Borrok, D.M., 2016. Isotope variations of dissolved Zn in the Rio Grande watershed, USA: the role of adsorption on Zn isotope composition. Earth Planet. Sci. Lett. 433, 293–302.
Wasylenki, L.E., Swihart, J.W., Romaniello, S.J., 2014. Cadmium isotope fractionation during adsorption to Mn oxyhydroxide at low and high ionic strength. Geochim. Cosmochim. Acta 140, 212–226.
Wiederhold, J.G., 2015. Metal stable isotope signatures as tracers in environmental geochemistry. Environ. Sci. Technol. 49, 2606–2624. https://doi.org/10.1021/es504683e.
Wiggenhauser, M., Bigalke, M., Imseng, M., Müller, M., Keller, A., Murphy, K., et al., 2016. Cadmium isotope fractionation in soil–wheat systems. Environ. Sci. Technol. 50, 9223–9231. https://doi.org/10.1021/acs.est.6b01568.
Wombacher, F., Rehkamper, M., 2004. Problems and suggestions concerning the notation of cadmium stable isotope compositions and the use of reference materials. Geostand. Geoanal. Res. 28, 173–178.
Xue, Z., Rehkämper, M., Horner, T.J., Abouchami, W., Middag, R., van de Flierd, T., et al., 2013. Cadmium isotope variations in the Southern Ocean. Earth Planet. Sci. Lett. 382, 161–172.
Yang, J., Li, Y., Liu, S., Tian, H., Chen, C., Liu, J., et al., 2015. Theoretical calculations of Cd isotope fractionation in hydrothermal fluids. Chem. Geol. 391, 74–82.
Yi, Q.T., Chen, Q.W., Hu, L.M., Shi, W.Q., 2017. Tracking nitrogen sources, transformation, and transport at a basin scale with complex Plain River networks. Environ. Sci. Technol. 51, 5396–5403.
Yu, K., Patrick, W.H., 2003. Redox range with minimum nitrous oxide and methane production in a rice soil under different pH. Soil Sci. Soc. Am. J. 67, 1952–1958.
Zhang, Y., Wen, H., Zhu, C., Fan, H., Luo, C., Liu, J., et al., 2016. Cd isotope fractionation during simulated and natural weathering. Environ. Pollut. 216, 9–17.
Zhu, M.Q., Frandsen, C., Wallace, A.F., Legg, B., Khalid, S., Zhang, H., et al., 2016. Precipitation pathways for ferrihydrite formation in acidic solutions. Geochim. Cosmochim. Acta 172, 247–264.
Zhu, C., Wen, H., Zhang, Y., Yin, R., Cloquet, C., 2018. Cd isotope fractionation during sulfide mineral weathering in the Fule Zn-Pb-Cd deposit, Yunnan Province, Southwest China. Sci. Total Environ. 616-617, 64–72.